

Article

Application of Portable Air Purifiers for Mitigating COVID-19 in Large Public Spaces

Zhiqiang (John) Zhai ^{1,*}, He Li ², Robert Bahl ³ and Keith Trace ³

¹ Department of Civil, Environmental and Architectural Engineering, University of Colorado at Boulder, 80309 Boulder, CO, USA

² School of Environmental Science and Engineering, Donghua University, 201620 Shanghai, China; 2151225@mail.dhu.edu.cn

³ Engineering & Facilities, Global Operations, , Marriott International, Inc., 20817 Bethesda, MD, USA; robert.bahl@marriott.com (R.B.); keith.trace@marriott.com (K.T.)

* Correspondence: john.zhai@colorado.edu; Tel.: +1-3034924699

Abstract: This study investigated, using validated computational fluid dynamics techniques, the actual performance of portable air purifiers for reducing the infection risks of airborne respiratory diseases such as COVID-19, by properly installing air purifiers in complicated large public spaces of primary concern, such as restaurants and ballrooms. The research results reveal that portable air purifiers with HEPA filtration provide an effective solution to help mitigate virus-carrying particles/droplets in large spaces where the central air conditioning system with HEPA filtration may not provide adequate dilution and/or effective ventilation. Deploying portable air purifier changes the local flow directions, and thus, reduces the cross-table airflows that may enhance the possibility of cross-infection. A field experiment was further conducted in a restaurant and a ballroom to verify the on-site performance. This study indicates that each space is unique in furniture, occupant and system layouts and capacities, and thus, requires individualized investigation of appropriate purifier number, capacities, and locations. Flexible solutions such as portable air purifiers are important and low-cost supplements to more elaborate solutions installed in central air systems.

Citation: Zhai, Z.; Li, H.; Bahl, R.; Trace, K. Application of Portable Air Purifiers for Mitigating COVID-19 in Large Public Spaces. *Buildings* **2021**, *11*, x. <https://doi.org/10.3390/xxxxx>

Keywords: portable air purifier; computational fluid dynamics; field experiment; public space; COVID-19

Academic Editor: Francesco Nocera

Received: 24 June 2021

Accepted: 26 July 2021

Published: date

Publisher's Note: MDPI stays neutral with regard to jurisdictional claims in published maps and institutional affiliations.



Copyright: © 2021 by the authors. Submitted for possible open access publication under the terms and conditions of the Creative Commons Attribution (CC BY) license (<https://creativecommons.org/licenses/by/4.0/>).

1. Introduction

In less than two years since the coronavirus disease 2019 (COVID-19) emerged, the pandemic has changed how we live, work, study, and interact as social distancing guidelines have led to a more virtual world, both personally and professionally. This became a more severe concern when scientific data supported the possibility that the COVID-19 virus may be transmitted by aerosols (so-called airborne transmission) [1]. It was highlighted that aerosol transmission may more likely occur in particular environments, such as indoor, crowded, and inadequately ventilated spaces, where the infected person(s) spend a relatively long period of time with others (e.g., over 30 min), such as classrooms, restaurants, choir practices, fitness classes, nightclubs, offices, and places of worship. Therefore, how to reduce the infection risks of airborne respiratory diseases in a public place becomes an urgent task for epidemiologists and public health experts.

The results in the survey study of Fabisiak et al. [2] indicated that 55% of respondents will be afraid to use public spaces after the COVID-19 lockdown. Restrictions on the use of public spaces and physical distancing have been key policy measures to reduce the transmission of COVID-19 and protect public health [3]. Despite the concerns and the difficulties faced throughout the pandemic, those who were committed to investigating the

new approaches to infection prevention demonstrated that they have managed to find promising solutions in their studies. Air purifiers, as traditional air pollution purification equipment, exhibit an excellent potential to reduce the infection risk of airborne transmission [4–7]. The Centers for Disease Control and Prevention (CDC) of the U.S. has continued to update guidance on airborne transmission, with the most recent update occurring on December 8th, 2020, which stated “Portable HEPA (high-efficiency particulate absorbing) filtration units that combine a HEPA filter with a powered fan system are a great option for auxiliary air cleaning.” In one example, the CDC concluded that “Adding the portable HEPA unit increased the effective ventilation rate and improved room air mixing. This resulted in over a 75% reduction in time for the room to be cleared of potentially-infectious airborne particles.” [4]. The American Society of Heating, Refrigerating and Air-Conditioning Engineers (ASHRAE) also provides some guidance on using portable air purifiers in confined spaces where ventilation is poor or where it is hard to keep social distancing, such as fitness centers, small public spaces, employee break rooms, or employee locker rooms [5]. Meanwhile, the U.S. Environmental Protection Agency (EPA) says “Consider using portable air cleaners to supplement increased Heating, ventilation, and air conditioning (HVAC) system ventilation and filtration, especially in areas where adequate ventilation is difficult to achieve. Directing the airflow so that it does not blow directly from one person to another reduces the potential spread of droplets that may contain infectious viruses” [6]. Furthermore, a few researchers have explored the use of air purifiers in specific rooms to reduce infection risks. For instance, Zhao et al. [7] studied and suggested the application of an air purifier as a supplementary protective measure in dental clinics during the COVID-19 pandemic. To improve indoor domestic environments in future pandemics, urgent action should be taken around indoor air quality (IAQ) to protect residents from respiratory ailments [8].

Air purifiers remove small particles/droplets that may carry viruses, whose efficiency is rated by the infiltration material. HEPA filters can theoretically remove at least 99.97% of dust, pollen, mold, bacteria, and any airborne particles with a size of 0.3 microns (μm). The diameter of 0.3 microns represents the worst case; particles of larger or smaller sizes are trapped with even higher efficiency. A pilot experiment showed that the flow of water mist into an air purifier inlet depended on the height of the source [9]. Proper design of air purifier installation (i.e., number, capacity, and location of units) is crucial to effectively remove airborne particles in spaces, particularly challenging in large public spaces. The actual performance of air purifiers can be affected by many factors, including indoor furniture and occupant layouts, existing mechanical system arrangements, and space openings such as doors, windows, connections, and leakages. This study explores the placement of two types of air purifiers (i.e., floor-standing air purifier (FAP) and table air purifier (TAP)) in two typical large public places (i.e., restaurant and ballroom) via both computational simulation and a field experiment to evaluate the performance of purifiers in mitigating the dispersion of particles/droplets released from the human mouth while breathing, talking or coughing.

2. Methodologies

The actual performance of air purifiers can be determined through either a physical test or a validated numerical experiment. While providing first-hand data, a physical test in a real space is often challenging, due to many uncontrollable variables, especially for pollutant/virus-related studies. A validated numerical experiment using computational flow dynamics (CFD) techniques provides a great alternative and is applied widely in the field. This study simulated the airflow pattern and contaminant transport in the spaces using a steady-state RANS (the Reynolds-Averaged Navier–Stokes equations) method. The RNG k - ϵ turbulence model in the commercial CFD code ANSYS Fluent 19.2 [10,11] was used to represent turbulence characteristics. The particle simulation assumed mono-dispersed non-interacting spherical particles. The momentum transfer from the particles to the air turbulence has a negligible impact on the flow [12–14].

Equations (1) and (2) describe the governing equations of the fluid phase [12]. The buoyancy effect of air is modeled with the Boussinesq approximation.

$$\frac{\partial}{\partial x_i}(v_i) = 0 \quad (1)$$

$$\rho \frac{\partial}{\partial x_i}(v_i v_j) = -\frac{\partial p}{\partial x_j} + \frac{\partial}{\partial x_i} \left[\mu \left(\frac{\partial v_i}{\partial x_j} + \frac{\partial v_j}{\partial x_i} \right) - \rho v_i' v_j' \right] \quad (2)$$

where v_j is the velocity component in three perpendicular coordinate directions ($x_j, j = 1, 2, 3$), m/s; ρ is the air density, kg/m³; p is the air pressure, Pa; μ is the kinematic viscosity coefficient of air; $v_i' v_j'$ is the Reynolds stress tensor.

When tracking the virus-carrying particles (in solid phase), the effect of the air drag force, gravity, and buoyancy were taken into account. The discrete particle model in Fluent (CFD-DPM) was used to track the individual particles [13]. The flow-governing equations of the solid phase single particle are described by Equations (3)–(6) [14]:

$$m_p \frac{d\vec{v}_p}{dt} = \vec{F}_D + m_p (\rho_p - \rho) \vec{g} / \rho_p \quad (3)$$

$$\vec{F}_D = \frac{\pi d_p^2 C_D (\vec{v} - \vec{v}_p) |\vec{v} - \vec{v}_p|}{8} \quad (4)$$

$$C_D = a_1 / \text{Re}_p + a_2 / \text{Re}_p^2 + a_3 \quad (5)$$

$$\text{Re}_p = \rho |\vec{v} - \vec{v}_p| D_p / \mu \quad (6)$$

where \vec{F}_D is the air drag force acting on the particle, N, the second term on the right side of Equation (3), represents gravity and buoyancy; m_p is the mass of the particle, kg; \vec{v}_p is the velocity vector of the particle, m/s; ρ_p is the particle density, kg/m³; v is the air velocity, m/s; v_p is the particle velocity, m/s; D_p is the particle diameter, m; μ is dynamic viscosity, N s/m²; a_1, a_2 , and a_3 are coefficients determined by Re_p .

3. Validation of the CFD Model

Exhaled air of an infected person is the primary source of contagious viruses. Exhaled air comes from various respiratory-related activities, such as breathing, coughing, singing, and talking. Accurate information on the release and diffusion process of exhaled airflow and particles is, thus, critical for the precise prediction of infectious disease transmission. This study focused on the talking scenario—the main concern during the dining and ball-room events when facial masks cannot be used. Studies showed that talking may release 2600 droplets per second at a speed of 1–5 m/s [15]. The range of the total airflow rate from a mouth when speaking is about 284–759 cm³/s [16]. Using an average of 500 cm³/s and assuming a mouth opening area at 1.8 cm² [16] leads to an average talking airflow speed of 2.77 m/s, which meets the particle image velocimetry (PIV) test result at the order of 3.1 m/s [17].

This study first conducted a test, via both physical experiment and CFD simulation, in the calm lab environment using a single table case with four occupants, including one infected person (Manikin 1) who intermittently talks, as shown in Figures 1 and 2. Table 1 lists the test case geometries. The thermal manikins of 70 Watt each have an average head/face temperature of 27 °C and an average body (with clothes) temperature of 22 °C. The space has no active air conditioning system, and the ambient room air, wall, ceiling, floor, and table surface temperatures are kept at 19 °C.

The mock-up physical experiment simulated the virus pollutant emitted from the mouth (with an inner size of 1.37 cm) of Manikin 1 by using stage fog (water-glycerin-mixture) as the tracer gas. The exit velocity of the fog from the mouth was controlled at around 2.77 m/s, representing a scenario where people are talking loudly. The supply time of the fog from the mouth is 20–25 s in the experiment and each test runs 2–5 min. A commercially available portable air purifier with a clean air delivery rate (CADR) of 166 m³/h was tested for the performance, with the most effective placement location as shown in Figures 1 and 2. The sizes of the portable air purifier are listed in Table 1.

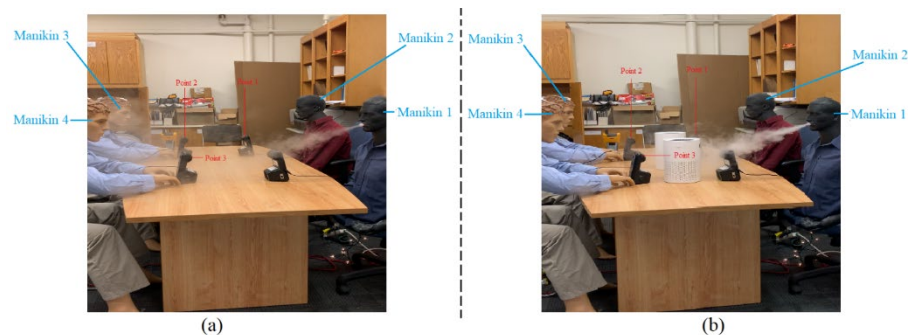


Figure 1. Lab experiment of the single table case: (a) without air purifiers; (b) with air purifiers.

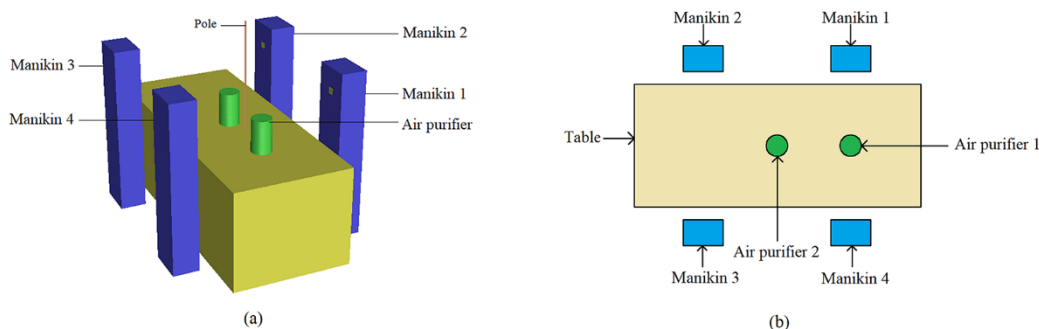


Figure 2. CFD model of the single table case: (a) axonometric view; (b) top view

Table 1. Geometries of the single table case.

Variable	Value
Table height	0.76 m
Table length	2.13 m
Table width	0.91 m
Distance between centers of manikin 1 and 4	1.3 m
Distance between centers of manikin 1 and 2	1.1 m
Floor to manikin mouth	1.1 m
Floor to manikin head	1.3 m
Air purifier height	0.25 m
Air purifier diameter	0.15 m
Ceiling height	3.1 m

Figure 2 illustrates the created CFD model for the single table case. The virus particle details simulated in CFD are presented in Table 2. The number of the particles released from the mouth was assumed as 5000 to ensure that the deviation of the particle statistical results is less than 1% [18]. Particles larger than 10 micron tend to drop quickly, while smaller particles tend to flow with air. The mean particle size during talking was 3 micron, which was thus used in the CFD model [19].

Table 2. Particle release conditions [16,20].

Variable	Value
Open area of the talking mouth	1.8 cm ²
Airflow rate from the talking mouth	500 cm ³ /s
Average talking airflow speed	2.77 m/s
Temperature of the airflow from the talking mouth	27 °C
Aerodynamic diameter of the particles	3 μm
Density of the particles	600 kg/m ³
Number of particles released from the talking mouth	5000

The CFD simulation first performed the grid sensitivity analysis to ensure the independence of the numerical results. Three numerical grids, 410,000, 770,000, and 1,000,000, were tested and compared using the normalized root mean square error (NRMSE) of the velocity at the pole shown in Figure 2 (30 points). The NRMSE of the velocity at the pole, respectively, between 410K and 1000K grids and between 770K and 1000K grids, are calculated as shown in Figure 3a. There is generally a great improvement in the error with the 770K grid, and the computational uncertainty is overall below 15%. By balancing the computational accuracy and cost, the 770,000 grid was, thus, chosen for the simulation. Among the 770,000 cells, fine grids were allocated around the mouths of the occupants, as shown in Figure 3b.

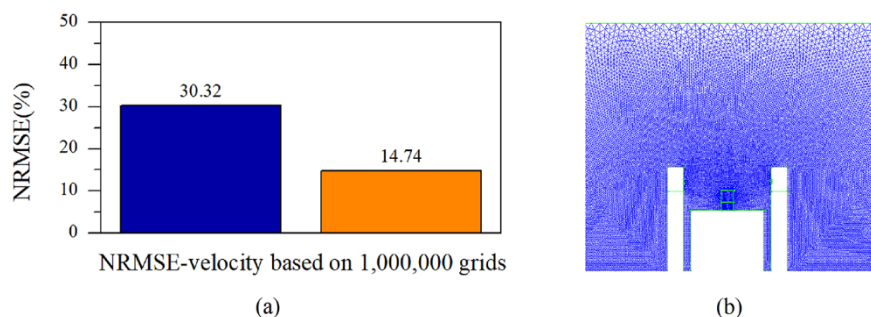


Figure 3. (a) NRMSE comparison between 410K/1000K grids and 770K/1000K grids; (b) Grid refinement with a 770K grid.

The mock-up experiment exhibits clearly, in Figure 1, that the fog exhaled from Manikin 1 can easily arrive at the face of Manikin 4, who is right across the table, and Manikin 3, who is diagonally across the table, when no air purifiers are used. When air purifiers were used, most of the fog exhaled from Manikin 1 was attracted towards the air purifiers, effectively containing the turbulent spread of the contaminant.

The similar dispersion processes of the particles were observed in the CFD simulation with and without air purifiers, as shown in Figure 4. Both mock-up test and CFD modeling indicate that the particle concentration at Manikin 4 (across the table from the source person) is less than those near Manikins 2 and 3, confirming the effectiveness of the air purifier placed between Manikin 1 and 4. Most of the particles can be directly removed by the purifier or blown away by the upward air from the top exit of the purifier.

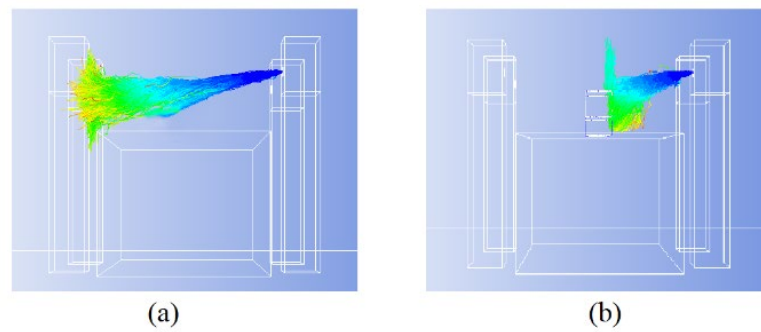


Figure 4. Dispersion of virus particles predicted by CFD: (a) without air purifier; (b) with air purifiers.

The comparison between simulation and experiment is quantitatively analyzed by calculating the reduction rate of the particle numbers ($M_{\text{reduction}}$) detected at the three locations of the sensors (Figure 1). $M_{\text{reduction}}$ can be defined as follows:

$$M_{\text{reduction},i} = \frac{M_{\text{without air purifier},i} - M_{\text{with air purifier},i}}{M_{\text{without air purifier},i}} \times 100\% \quad (7)$$

where $M_{\text{without air purifier},i}$ is the number of particles sensed at the i th point ($i = 1, 2, 3$) for the case without air purifiers and $M_{\text{with air purifier},i}$ is the number of particles sensed at the i th points ($i = 1, 2, 3$) for the case with air purifiers. Figure 5 compares the results obtained from the simulation and test.

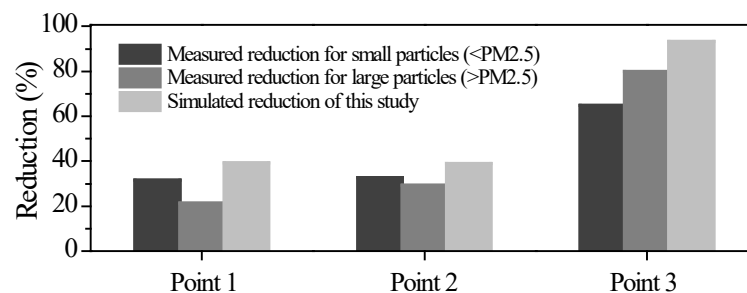


Figure 5. Comparison of simulated and measured reduction rate of particle numbers.

Both the qualitative and quantitative comparisons between the mock-up experiment and the CFD simulation verify that the simulation model can project reasonable results to track the virus-carrying particles' trajectories. Therefore, a sophisticated CFD model that is made of many similar tables and occupants should be able to predict the transportation of the virus-carrying particles in a complex large built environment.

4. CFD Simulation and Analysis of Large Public Spaces

This study used the validated CFD model to simulate a restaurant and a ballroom as two representative public places to evaluate the effect of using portable air purifiers to mitigate COVID-19 in large spaces. Steady-state air circulation conditions were simulated to determine the best location, air exchange rate requirement, and quantity of air purifiers. The restaurant and the ballroom are conditioned with a central HVAC system, which supplies clean air from the ceiling inlets and exhausts room air from the ceiling/upper-level outlets. To assess the actual performance of the commercial purifier on mitigating COVID-19, virus-carrying particles released from one infected occupant in the restaurant and the ballroom were simulated and tracked, using the same settings as used in the validation

model. A grid sensitivity analysis was also performed to ensure the accuracy of the numerical results. The suitable total grid cells were determined to be about 650,000 and 4,470,000 for the restaurant and the ballroom, respectively.

4.1. Restaurant Case

4.1.1. Case Description

A CFD model (shown in Figure 6) of a restaurant (total space area 370 m²) was built in ICMCFD (Integrated Computer Engineering and Manufacturing code for CFD). The specifications of the restaurant are summarized in Table 3.

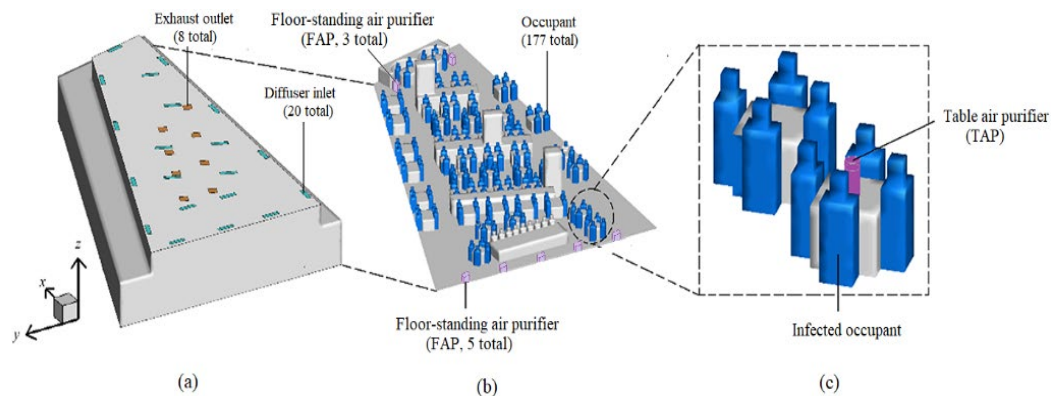


Figure 6. Computer model and components of the restaurant: (a) the placement of exhaust outlets and diffuser inlets; (b) the locations of all occupants; (c) the location of the infected occupant

Table 3. Restaurant specifications.

Object	Dimensions	Boundary Conditions
Diffuser inlet	1.22 × 0.30 m ²	T _{in} = 17.6 °C
Table	0.87 × 0.87 × 0.75 m ³	Adiabatic
Exhaust outlet	0.61 × 0.61 m ²	T _{ex} = 20 °C
Diner body	0.3 × 0.43 × 1.3 m ³	27 °C
light		10.7 W/m ²
Air change rate		5 times/h
Supply air velocity		0.3429 m/s

To evaluate the effectiveness of air purifiers on reducing the potential infection risk to the healthy occupants, floor-standing air purifier (FAP), and table air purifier (TAP) were arranged in the restaurant. As listed in Table 4, two kinds of commercial purifiers [21,22] were employed to purify indoor air. Indoor air flows into the purifier from the side of the purifier and then flows out from the top of the purifier. Eight FAPs are placed at both ends of the restaurant (Figure 6). The restaurant was operated at full capacity, with 177 occupants, in which one was the virus-carrier, as shown in Figure 6c. One TAP was placed at the center of the dining table occupied by the infected occupant.

Table 4. Purifier specifications.

	Floor-Standing Air Purifiers (FAP)	Table Air Purifier (TAP)
Dimensions	0.56 × 0.33 × 0.61 m ³	0.2 × 0.2 × 0.42 m ³
Inlet size	0.13 m ²	0.19 m ²
Outlet size	0.05 m ²	0.03 m ²
Clean air delivery rate	554.4 m ³ /h	197.7 m ³ /h

Particle release conditions were the same as those in the validation case (Table 2). Particle trajectories were investigated, respectively, under three ventilation conditions: (1) central air-conditioning system (CA); (2) central air-conditioning system with floor-standing air purifiers (CAF); and (3) central air-conditioning system with both floor-standing air purifiers and table air purifier (CAFT), to analyze the fate of the particles exhaled from the infected occupant.

4.1.2. Flow Field and Particle Trajectory Analysis

The movement of airflow is deterministic to the particle trajectory. Under the three ventilation conditions (i.e., CA, CAF, and CAFT), the velocity vector of airflow near the infected occupant (Figure 6c) at the height of the breathing zone ($Z = 1.1$ m) is shown in Figure 7. Installing portable air purifiers changes the local flow directions and mitigates the cross-table airflow that may cause cross-infection. The table unit, with proper capacity, displays explicit and favorable air inflow towards the purifier. The dispersion processes of the particles under the three flow fields are shown in Figure 8. The flow paths of the viral particles exhaled from the infected occupant are different for the three ventilation conditions. The particles under the CA system can easily arrive at the breathing zone of the opposite occupant. For the CAF system, the particles move up first and are then sucked by the floor-standing air purifier placed at the back, which purifies the air with the particles. The CAFT system presents a better purification performance, because most of the particles are directly sucked into the table purifier as well as pushed upwards due to the strong upward outflow from the top air exit of the unit.

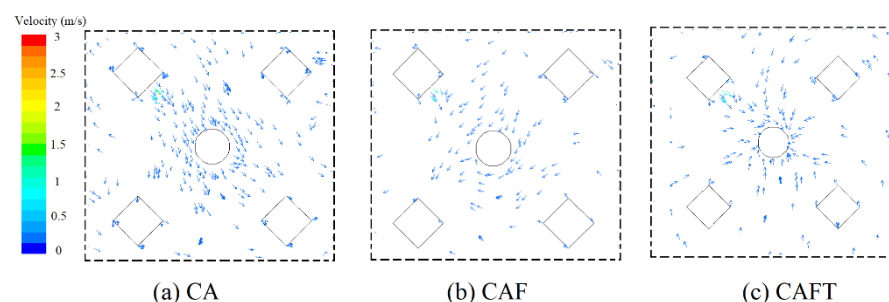


Figure 7. The velocity vector of airflow near the infected occupant under different ventilation conditions ($Z = 1.1$ m).

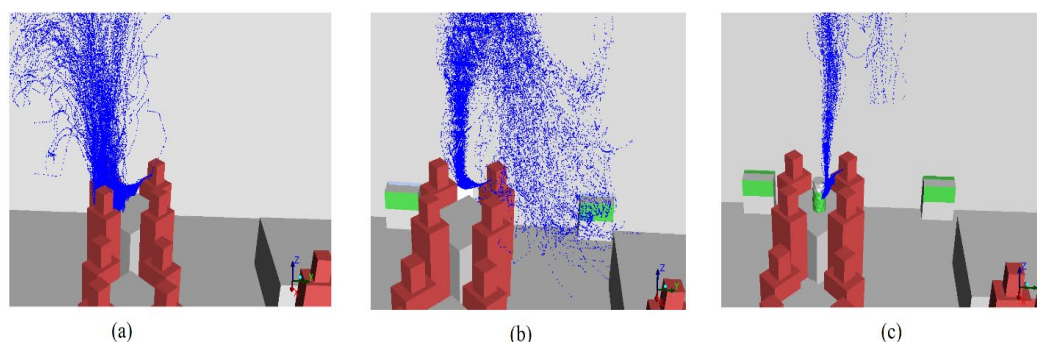


Figure 8. The dispersion processes of virus-carrying particles under three ventilation conditions: (a) CA; (b) CAF; (c) CAFT.

4.1.3. Fate Analysis of the Virus-Carrying Particles Exhaled from the Infected Occupant

Figure 9 compares quantitatively the percentage of particles that are, respectively, discharged from the central exhausts, purified by the purifiers, and deposited on different surfaces under different ventilation conditions. Particles released from the mouth of the

infectors are convenient to spread in the horizontal direction under the central air-conditioning system (CA), especially at the height of the breathing zone. A small fraction of the particles is discharged through the exhaust outlets under CA. Most of them are spread out in the indoor space and then deposited on the diners (33%), the table (25%), the ground (25%), and the walls (11%). The floor-standing purifiers (FAP) can purifier 28% of the particles while increasing the particle deposition on the walls (48%) due to the redirected air inflow and outflow around the purifiers. The particle concentration at the height of the breathing zone under the CAF system is smaller than that under the CA system. With the CAF system, most of the viral particles are purified by the table air purifier (TAP)—about 76% of particles can be purified by TAP, a remarkable performance in purifying particles.

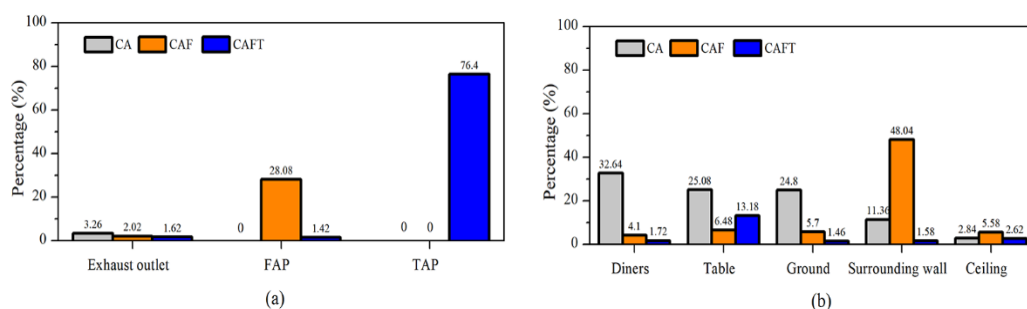


Figure 9. Particle distribution statistics for CA, CAF, and CAFT, respectively: (a) percentage of particles discharged from the exhaust outlets and purified by the purifiers; (b) percentage of particles deposited on different surfaces.

To assess the quantitative performance of air purifiers on reducing infection risks, the reduction rate of the number of particles deposited on the surrounding occupants ($N_{\text{reduction}}$) is calculated by comparing the cases with and without air purifiers. $N_{\text{reduction}}$ is defined as in Equation (8):

$$N_{\text{reduction}} = \frac{N_{\text{without air purifiers}} - N_{\text{with air purifiers}}}{N_{\text{without air purifiers}}} \times 100\% \quad (8)$$

where $N_{\text{without air purifiers}}$ is the number of particles deposited on the occupants for the case without air purifiers, $N_{\text{with air purifiers}}$ is the number of particles deposited on the occupants for the case with air purifiers. Using Equation (8) and the data in Figure 9, $N_{\text{reduction}}$ is obtained for the CAF and CAFT cases, respectively, compared to the CA case, as seen in Table 5. $N_{\text{reduction}}$ of CAFT is greater than that of CAF, which verifies that the table air purifier (TAP) has a superior performance in mitigating the infection risk. The optimal location of the air purifier will be in proximity where people are seated, congregated or in a queue. The study of Mousavi et al. [23] indicated that the best location of a single portable air purifier unit is inside the isolation room and near the patient's bed. The result of this study is, thus, consistent with the suggestion in the literature [23].

Table 5. $N_{\text{reduction}}$ for CAF and CAFT as compared to CA.

	CAF	CAFT
$N_{\text{reduction}}$	87.4%	94.7%

4.2. Ballroom Case

4.2.1. Case Description

Section 4.1 concludes that the table air purifier (TAP) provides an effective means to help mitigate airborne transmission of pathogens in the restaurant. TAP was further investigated to evaluate its application for one larger event (i.e., ballroom). The CFD model of the ballroom (total space area 3200 m²) built in ICMCFD is shown in Figure 10 and the

specifications of the ballroom are summarized in Table 6. The ballroom is full of diners (1320 total), with one of them infected (Figure 10). One TAP is placed at the center of the dining table occupied by the infected person. Purifier specifications and particle release conditions, respectively, are shown in Tables 4 and 2. Particle trajectories were investigated, respectively, under two ventilation conditions: (1) central air-conditioning system (CA-Ballroom) and (2) central air-conditioning system with table air purifier (CAT), to analyze the fate of the viral particles exhaled from the infected occupant in the ballroom.

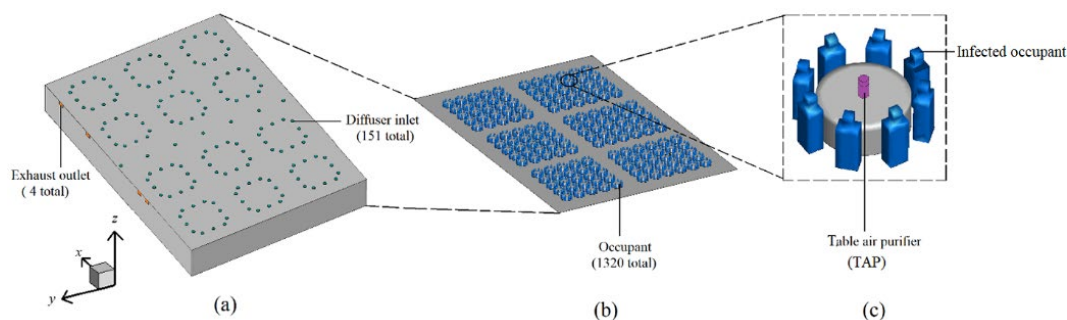


Figure 10. Computer model and components of the ballroom : (a) the placement of exhaust outlets and diffuser inlets; (b) the locations of all occupants; (c) the location of the infected occupant

Table 6. Ballroom specifications.

Object	Dimensions	Boundary Conditions
Inlet diffuser diameter	0.8 m	$T_{in} = 17.6 \text{ }^{\circ}\text{C}$
Table diameter	1.82 m	Adiabatic
Exhaust outlet	$1.58 \times 1.1 \text{ m}^2$	$T_{ex} = 20 \text{ }^{\circ}\text{C}$
Diner body	$0.3 \times 0.43 \times 1.3 \text{ m}^3$	$27 \text{ }^{\circ}\text{C}$
Light		10.7 W/m^2
Air change rate		5 times/h
Supply air velocity		0.4672 m/s

4.2.2. Flow Field and Particle Trajectory Analysis

The velocity vector of airflow at the height of the breathing zone ($Z = 1.1 \text{ m}$) at the table with the infector is shown in Figure 11, respectively, for the cases under two ventilation conditions (i.e., CA-Ballroom and CAT). The table air purifier changes the local flow directions, displaying explicit and favorable air inflow towards the purifier. The dispersion processes of virus particles under the two flow fields are shown in Figure 12. The spread range of the viral particles for the CA-Ballroom system is much larger than that for the CAT system, even reaching the neighboring tables. These particles, however, are confined around the purifier with the CAT system due to the negative pressure effect, which avoids the viruses' large-scale spread. Although the particles are not fully attracted by the table purifier, the dispersion of the virus at the horizontal plane has been reduced significantly by using TAP.

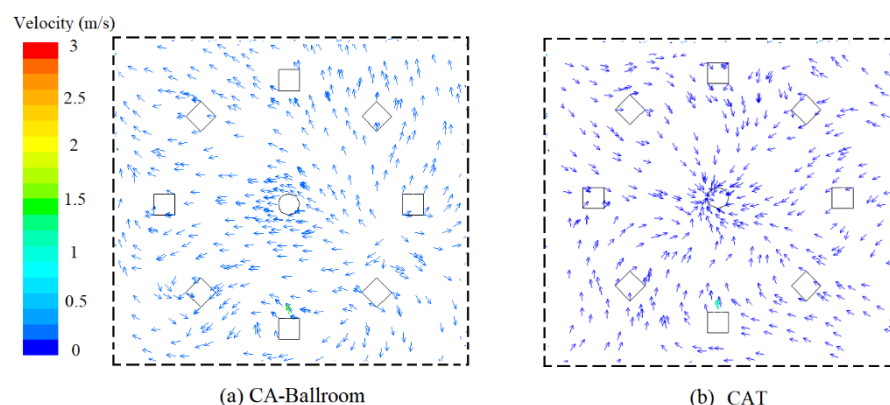


Figure 11. The velocity vector of airflow at the height of the breathing zone ($Z = 1.1$ m) at the table with the infector under two ventilation conditions.

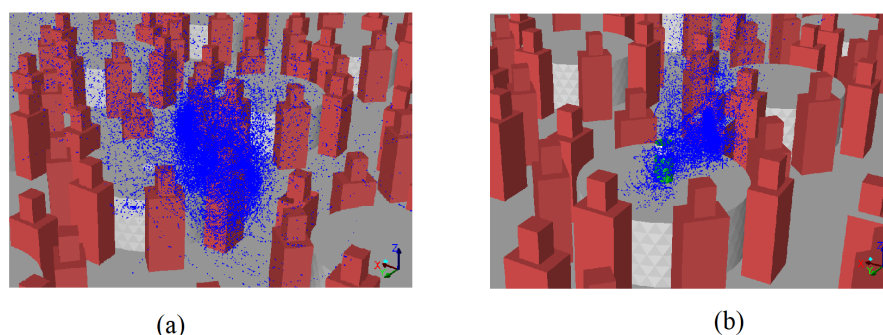


Figure 12. The dispersion processes of viral particles under two ventilation conditions: (a) CA-Ballroom; (b) CAT.

4.2.3. Fate Analysis of the Virus-Carrying Exhaled from the Infected Occupant

Figure 13 compares the percentage of the particles that are, respectively, exhausted from the central air outlets, purified by the purifier, and deposited on different surfaces under the two ventilation conditions. Although only 12% of particles were purified by the TAP, which is attributed to the longer distance between the unit and the infector (the larger diameter of the dining table) compared to the restaurant case, the TAP helps reduce the deposition of particles on the occupants (potential cross-infection risk) from 29% to 11%. More particles were pushed up towards the ceiling (49%) due to the upward exit flow of the TAP, rather than distributing horizontally, which is a potential cause of cross-infection.

We obtained 60.3% of $N_{\text{reduction}}$ for the CAT compared to CA-Ballroom using Equation (8) and the data in Figure 13. While this number is lower than that in the restaurant, it is still promising, especially considering the small size and capacity of the purifier. The arrangement of a table air purifier can be as effective as more elaborate solutions installed in the HVAC system at a lower cost. Flexible solutions, such as portable air purifiers, can be redeployed throughout the property as needed.

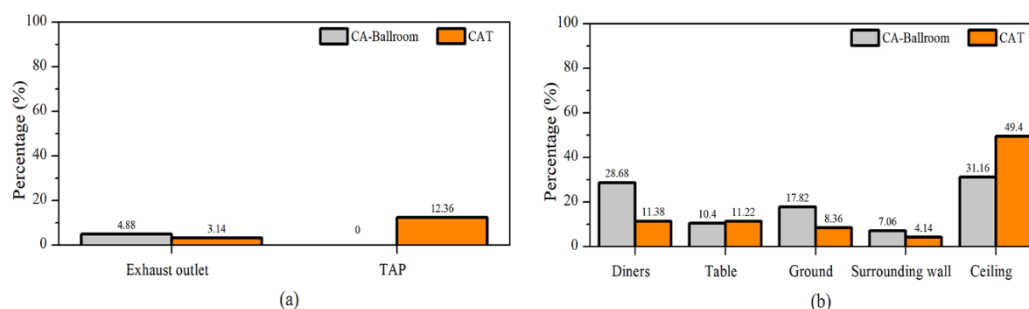


Figure 13. Particle distribution statistics for CA-Ballroom and CAT: (a) percentage of particles discharged from the exhaust outlets and purified by the purifier; (b) percentage of particles deposited on different surfaces.

5. Field Experiment and Analysis of Large Public Spaces

CFD simulation indicates that the installation of portable air purifiers can be an effective measure to reduce the infection risks of aerosol transmission in large public spaces. To verify the actual performance of the purifiers in the real operation conditions, this study further conducted the field experiment in two large public spaces (restaurant and ballroom). A commercial purifier (Blueair-411PACF105372) of 197.7 m³/h was installed and tested in the experiment. Stage fog (water-glycerin-mixture) was used as a tracer gas released from the mouth of the infector. The distribution of the fog was recorded as shown in Figure 14, under the central air-conditioning system with and without a purifier. Most of the fog exhaled from the infector was sucked into the table air purifier, and the distributed area of the fog with the table purifier is much more confined than that without the purifier, similar to what was found in CFD simulation.

Similar performance was observed for the test in the ballroom (Figure 15). Although most of the released fog was not directly sucked in by the table purifier, the spread of the fog to the surrounding area was slowed down due to the table purifier. It appears that the negative pressure area around the table purifier cannot completely cover the infected occupant when the unit is placed at the center of a large table. A more powerful table purifier will be required to provide a better performance.



Figure 14. The dispersion processes of stage fog (a) without and (b) with purifier in a restaurant.

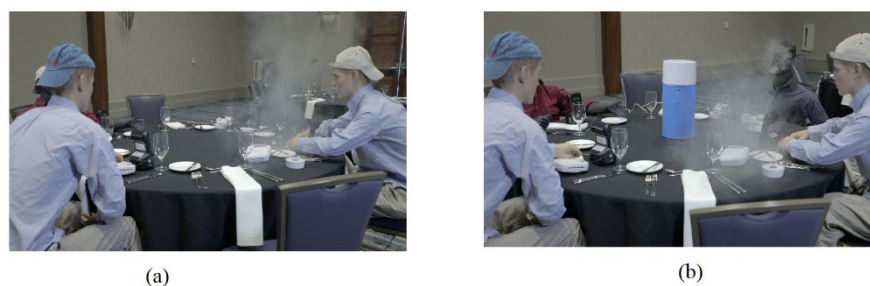


Figure 15. The dispersion processes of stage fog (a) without and (b) with purifier in a ballroom.

6. Conclusions

COVID-19 is a test like no others. Never before have the lives of so many people around the world been affected at this scale or speed. In this study, the air purifier, as a facility recommended by organizations such as the US CDC and ASHRAE, was investigated for its actual performance in reducing the infection risks of the virus. The installation of air purifiers in two typical public places (i.e., restaurant and the ballroom) was studied, as compared to the use of the existing central air-conditioning systems. Validated CFD models were created and applied to explore the qualitative and quantitative performance of the portable air purifiers, which was further verified by a qualitative field experiment in the actual restaurant and ballroom.

The research outcomes reveal that the central air condition system only exhausts a small fraction of the particles released from the mouth of the infector, and most of the particles are spread out indoors and ultimately deposited on occupants, tables, equipment, ground, and walls. Both floor-standing and table air purifiers, with proper locations and capacities, can effectively attract room air to flow towards the purifiers and, therefore, clean the “contaminated” air. Similar behavior and performance were observed in the actual restaurant and the ballroom, while the results indicate that each space is unique in geometry, layout, and system and, thus, needs to be addressed individually. Flexible solution allows the redeployments of the cleaning devices throughout the property as needed. Portable air purifiers with HEPA filtration provide an effective means to help mitigate the airborne transmission of pathogens, which can be as effective as more elaborate solutions installed in the HVAC systems at a lower cost.

Author Contributions: Conceptualization, Zhiqiang (John) Zhai, Robert Bahl and Keith Trace; Data curation, He Li; Formal analysis, Zhiqiang (John) Zhai, He Li, Robert Bahl and Keith Trace; Funding acquisition, Zhiqiang (John) Zhai, Robert Bahl and Keith Trace; Investigation, Zhiqiang (John) Zhai, He Li, Robert Bahl and Keith Trace; Methodology, Zhiqiang (John) Zhai, He Li and Robert Bahl; Project administration, Zhiqiang (John) Zhai, Robert Bahl and Keith Trace; Resources, Zhiqiang (John) Zhai, Robert Bahl and Keith Trace; Software, He Li; Supervision, Zhiqiang (John) Zhai and Robert Bahl; Validation, Zhiqiang (John) Zhai and He Li; Visualization, He Li; Writing – original draft, Zhiqiang (John) Zhai and He Li; Writing – review & editing, Zhiqiang (John) Zhai.

Funding: This work was supported by Marriott International, Inc.

Institutional Review Board Statement: Not applicable

Informed Consent Statement: Not applicable **Data Availability Statement:** Not applicable

Conflicts of Interest: The authors declare no conflict of interest.

References

1. Klompas, M.; Baker, M.A.; Rhee, C. Airborne Transmission of SARS-CoV-2: Theoretical Considerations and Available Evidence. *JAMA* **2020**, *324*, 441–442.
2. Fabisiak, B.; Jankowska, A.; Kłos, R. Attitudes of Polish seniors toward the use of public space during the first wave of the COVID-19 pandemic. *Int. J. Environ. Res. Public Health* **2020**, *17*, 8885.
3. Honey-Rosés, J.; Anguelovski, I.; Chireh, V.K.; Daher, C.; Konijnendijk van den Bosch, C.; Litt, J.S.; Mawani, V.; McCall, M.K.; Orellana, A.; Oscilowicz, E.; et al. The impact of COVID-19 on public space: An early review of the emerging questions—design, perceptions and inequities. *Cities Health* **2020**, 1–17, doi:10.1080/23748834.2020.1780074.
4. CDC. Ventilation in Buildings: <https://www.cdc.gov/coronavirus/2019-ncov/community/ventilation.html> (accessed on 27 July 2021).
5. ASHRAE. *ASHRAE Position Document on Filtration and Air Cleaning*; **2021**.
6. EPA. Air Cleaners, HVAC Filters, and Coronavirus (COVID-19): <https://www.epa.gov/coronavirus/air-cleaners-hvac-filters-and-coronavirus-covid-19> (accessed on 17 March 2021).
7. Zhao, B.; An, N.; Chen, C. Using an air purifier as a supplementary protective measure in dental clinics during the coronavirus disease 2019 (COVID-19) pandemic. *Infect. Control Hosp. Epidemiol.* **2020**, *42*, 493.
8. Domínguez-Amarillo, S.; Fernández-Agüera, J.; Cesteros-García, S.; González-Lezcano, R.A. Bad air can also kill: Residential indoor air quality and pollutant exposure risk during the covid-19 crisis. *Int. J. Environ. Res. Public Health* **2020**, *17*, 7183.
9. Ham, S. Prevention of exposure to and spread of COVID-19 using air purifiers: Challenges and concerns. *Epidemiol. Health Korean Soc. Epidemiol.* **2020**, *42*, e2020027.

10. Zhang, Z.; Zhang, W.; Zhai, Z.J.; Chen, Q.Y. Evaluation of Various Turbulence Models in Predicting Airflow and Turbulence in Enclosed Environments by CFD : Part 2—Comparison with Experimental Data from Literature. *HVAC&R Res.* **2007**, *13*, 871–886.
11. Chen, Q.; Zhai, Z. The use of CFD tools for indoor environmental design. In *Advanced Building Simulation*; Spon Press: New York, NY, USA, 2004; pp. 119–140.
12. Chen, X.; Zhong, W.; Sun, B.; Jin, B.; Zhou, X. Study on gas/solid flow in an obstructed pulmonary airway with transient flow based on CFD-DPM approach. *Powder Technol.* **2012**, *217*, 252–260.
13. Holmberg, S. Modelling of the indoor environment—Particle dispersion and deposition. *Indoor Air* **1998**, *8*, 113–122.
14. Li, H.; Zhong, K.; Zhai, Z. Investigating the influences of ventilation on the fate of particles generated by patient and medical staff in operating room. *Build. Environ.* **2020**, *180*, 107038.
15. Asadi, S.; Wexler, A.S.; Cappa, C.D.; Barreda, S.; Bouvier, N.M.; Ristenpart, W.D. Aerosol emission and superemission during human speech increase with voice loudness. *Sci. Rep.* **2019**, *9*, 2348.
16. Gupta, J.K.; Lin, C.; Chen, Q. Characterizing exhaled airflow from breathing and talking. *Indoor Air* **2010**, *20*, 31–39.
17. Chao, C.Y.; Wan, M.P.; Morawska, L.; Johnson, G.R.; Ristovski, Z.D.; Hargreaves, M.; Mengersen, K.; Corbett, S.; Li, Y.; Xie, X.; et al. Characterization of Expiration Air Jets and Droplet Size Distributions Immediately at the Mouth Opening. *J. Aerosol. Sci.* **2009**, *40*, 122–133.
18. Fang, T.; Wang, S.; Zhang, T. Modeling Particle Filtration Performance of A Breathing Wall. *J. Liaoning Univ. Sci. Ed.* **2013**, *40*, 125–131.
19. Sun, C.; Zhai, Z. The Efficacy of Social Distance and Ventilation Effectiveness in Preventing COVID-19 Transmission. *Sustain. Cities Soc.* **2020**, *62*, 102390.
20. Li, H.; Zhong, K.; Zhai, Z. Potential risk analysis of medical staff when performing endotracheal intubation in negative pressure isolation ward. *Indoor Built Environ.* **2021**, doi:10.1177/1420326X20979015.
21. Honeywell True HEPA Bluetooth Smart Air Purifier With Allergen Remover, HPA8350B: <https://www.honeywell-store.com/store/products/honeywell-hepa-bluetooth-smart-air-purifier-hpa8350b.htm> (accessed on 1 March 2021).
22. Blueair Blue Pure 411+ Air Purifier for Home: https://www.amazon.com/Blueair-Purifier-Washable-Pre-Filter-Allergens/dp/B085B4V3DN/ref=sr_1_12?dchild=1&keywords=portable+purifier&qid=1602947139&s=home-garden&sr=1-12 (accessed on 1 March 2021).
23. Mousavi, E.S.; Pollitt, K.J.; Sherman, J.; Martinello, R.A. Performance analysis of portable HEPA filters and temporary plastic anterooms on the spread of surrogate coronavirus. *Build. Environ.* **2020**, *183*, 107186.